CATHENA Simulation of Thermosiphoning in a Pressurized-Water Test Facility

J.P. Mallory
Wardrop Engineering Consultants
77 Main Street
Winnipeg, Manitoba R3C 3H1
P.J. Ingham
Atomic Energy of Canada Limited
Whiteshell Nuclear Research Establishment
Pinawa, Manitoba R0E 1L0

Abstract

Under some postulated accident conditions, decay heat is removed from a reactor core by 2-phase natural circulation or 'thermosiphoning' of the primary coolant. To assess the ability of the computer code CATHENA (Canadian Algorithm for THermalhydraulics Network Analysis, formerly ATHENA) to predict such events, simulations were performed of thermosiphoning tests conducted in the RD-14 facility at the Whiteshell Nuclear Research Establishment. Predictions for 3 test conditions are presented. Generally, the predicted behaviour agrees with the observed results. Non-oscillating 2-phase thermosiphoning, and the onset of oscillatory flow, are well predicted. Channel heater temperature behaviour is also well predicted. In some instances, the predicted oscillating period tends to be longer than that observed in the experiment, and the predicted amplitude larger than the experimental results. It is speculated that the simplified heat transfer boundary conditions, used to represent the steam generators secondary side, are mainly responsible for these discrepancies.

Résumé

Dans certaines conditions d'accidents hypothétiques, la chaleur de désintégration est évacuée du coeur d'un réacteur par la circulation naturelle à deux phases ou 'processus de thermosiphon' du caloporteur primaire. Pour évaluer la capacité du programme de calcul CATHENA (Canadian Algorithm for THErmalhydraulics Network Analysis, appelé avant ATHENA) de prédire de tels évènements, on a simulé des essais de circulation naturelle (processus de thermosiphon) effectués dans l'installation RD-14 de l'Établissement de recherches nucléaires de Whiteshell. On présente les prédictions pour trois conditions d'essais. En général, le comportement prédit correspond aux résultats observés. La prédiction de la circulation naturelle à deux phases (processus de thermosiphon) non oscillante et du début de l'écoulement oscillatoir est bonne. La prédiction du comportement thermique des réchauffeurs de canaux est bonne également. Dans certains cas, la période d'oscillation tend à être plus longue que celle observée lors des essais et l'amplitude prédite plus grande que les résultats d'essais. On suppose que les conditions aux limites simplifiées de transfert de chaleur, qui servent à représenter le circuit secondaire des générateurs de vapeur, sont les causes principales de ces différences.

Introduction

The computer code CATHENA has been developed primarily to analyze postulated loss-of-coolant accidents (LOCA) scenarios for CANDU™ nuclear reactors. Under some conditions, decay heat removal from the core is by single or 2-phase thermosiphoning. It is important to determine that decay heat can be adequately removed in this situation.

Tests were conducted in the RD-14 facility to examine the thermosiphoning flow behaviour as a function of the initial primary fluid inventory. These experiments provide data which can be used to assess the predictive capability of various thermalhydraulic codes.

In this paper, results are presented for 3 of the test conditions examined. The test facility, the experiments, and the code are described briefly. The experiments and the CATHENA simulations are discussed in more detail.

Experiments

Facility Description

Figure 1 shows a simplified flow diagram of the RD-14 thermalhydraulic test facility. The emergency coolant injection system and the blowdown lines were not used in these experiments. The facility is a

Keywords: after-heat removal, natural convection, computerized simulation.

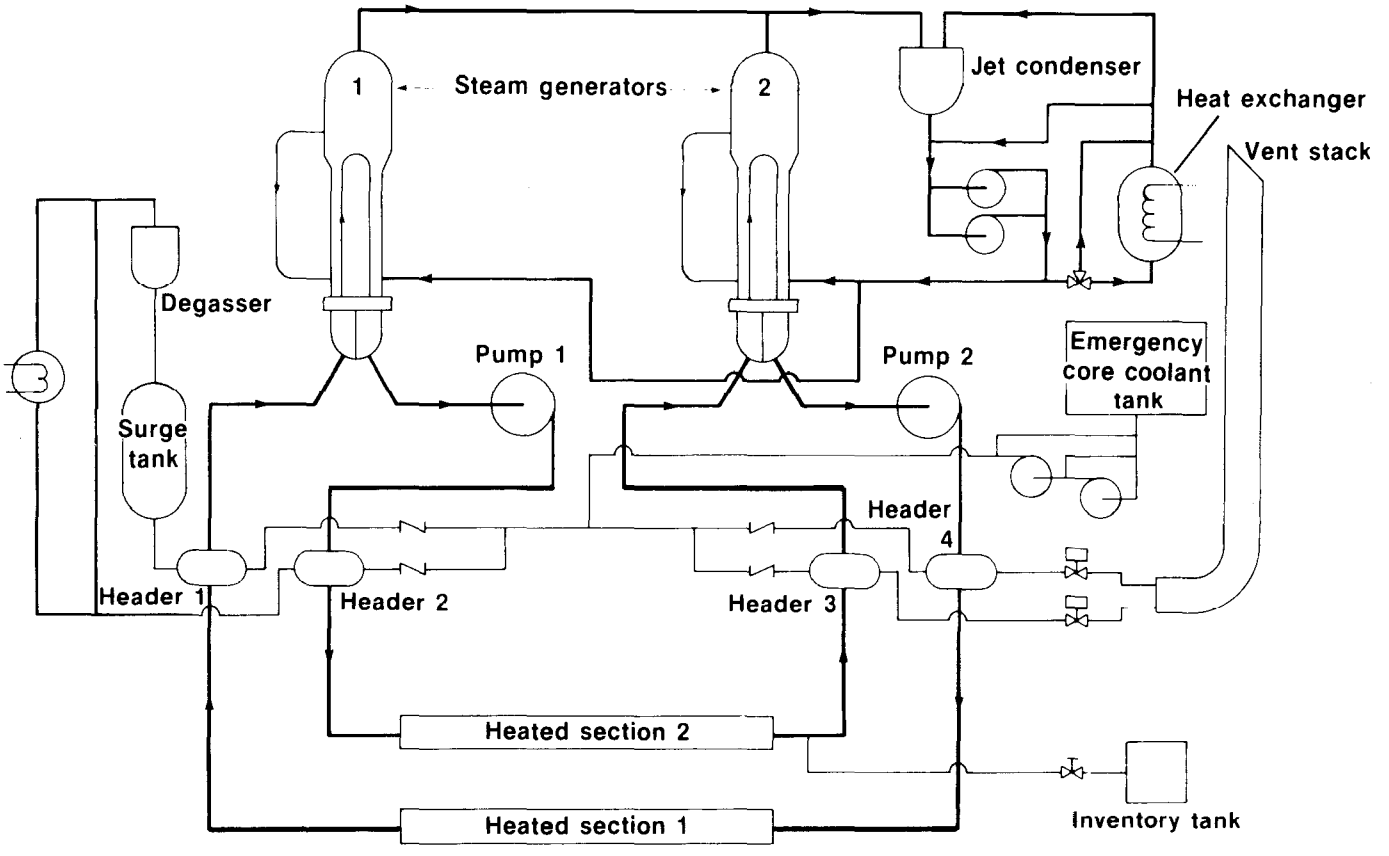

Figure 1 Schematic diagram of the RD-14 facility.

pressurized-water loop (10 MPa nominal) with the basic 'figure-of-eight' geometry of a CANDU™ reactor. It has two 6-metre-long, 5.5 MW horizontal channels, connected to end-fitting simulators representing 2 passes through a reactor core. Each channel contains 37 electrically heated fuel-element simulators of almost the same heat capacity as reactor fuel. Heat is removed from the primary circuit through 2 recirculating U-tube-type steam generators with internal pre-heaters and external downcomers. Primary fluid circulation is provided by 2 high-head centrifugal pumps, which generate channel flowrates similar to a single reactor channel.

The heated channels, steam generators, pumps, and headers are arranged to obtain a 1:1 vertical scale of a typical CANDU reactor. The steam generators are also scaled approximately 1:1 with those of a typical CANDU steam generator in terms of tube diameter, mass, and heat flux, to achieve reactor-like conditions within them. The facility is designed to produce the same fluid mass flux, transit time, pressure, and enthalpy conditions in the primary system as those in a typical reactor under both forced and natural circulation. Major loop parameters of RD-14 and a typical reactor are shown in Table 1.

Primary side pressure is controlled by a surge tank equipped with an electrical heater. Secondary side pressure is controlled by a jet condenser in which steam is condensed by contact with cold water. The cooled condensate is returned to the steam generator as feedwater.

Fluid removed from the primary circuit, for these thermosiphoning tests, is cooled and stored in an inventory tank. Level monitoring of the inventory tank provides a record of the quantity of primary fluid removed.

Loop instrumentation consists of multi-beam gamma-ray densitometers for fluid density measurements, differential and gauge pressure transducers, thermocouples, and resistance temperature detectors. Volumetric flowrates are measured using turbine flow meters.

Experimental Procedure

Before each experiment, the RD-14 facility was evacuated, filled with distilled water, degassed, and final instrument calibrations were completed. The loop was then brought to conditions of stable, single-phase, natural circulation of the primary fluid at the preselected heated section power, and primary and secondary pressures. After the pressurizer was isolated and approximately 10 seconds of steady state data collected, the experiment was begun. Two-phase conditions were induced by controlled, intermittent draining of

Table 1: Comparison of Characteristics of RD-14 with Those of a Typical CANDU Reactor

Characteristic	*RD-14*	*Typical CANDU reactor*
Operating Pressure (MPa)	10	10
Loop volume (m^3)	0.9514	57.0
Loop piping I.D. (m)	0.074	varies
Heated sections	indirect heated 37-rod bundles	nuclear fuel 37-element bundle
Length (m)	6	12 × 0.5
Rod diameter (m)	0.0131	0.0131
Flow tube diameter (m)	0.1034	0.1034
Power (kW / channel)	5500	5410
Pumps:	single-stage	single-stage
Impeller diameter (m)	0.381	0.813
Rated flow (kg / s)	24	24 (max / channel)
Rated head (m)	224	215
Specific speed	565	2000
Steam generators	recirculating U-tube	recirculating U-tube
Number of tubes	44	37 / channel
Tube diameter I.D. (m)	0.01363	0.01475
Secondary heat-transfer area (m^2)	41	32.9 / channel
Heated section-to-boiler top elevation difference (m)	21.9	21.9

primary fluid from the outlet of heated section 2 into an inventory tank. A typical draining sequence can be seen in Figure 5. In the first 5 draining operations, approximately 2% of the initial loop inventory of 0.9514 m^3 (excluding pressurizer volume) was removed. In each of the subsequent draining operations, 10% was removed. In the experiments described in this paper, intermittent draining was continued until the heater element sheath temperatures reached 600°C.

Two different secondary side pressures were chosen. The higher pressure, 4.6 MPa, is representative of reactor secondary pressure following a postulated loss-of-class-IV power event. The lower pressure, 0.2 MPa, is representative of a postulated loss-of-primary-coolant, design-basis earthquake or main steam-line break event. At each secondary side pressure, a high- and a low-power test was conducted. Two of the tests were checked for repeatability, with good results. Table 2 contains a summary of the test conditions. A more detailed discussion of the experimental results is available [Krishnan 1987].

CATHENA Simulations

Code Description

CATHENA is a 1-dimensional thermalhydraulics computer code developed at WNRE, primarily to analyze postulated loss-of-coolant accident scenarios for CANDU nuclear reactors. The code uses a non-equilibrium, 2-fluid thermalhydraulic model to describe fluid flow. Conservation equations for mass, momentum, and energy are solved for each phase (liquid and vapour). Interphase transfer of mass, momentum, and energy is handled by a set of flow-regime-dependent constitutive relations. As well, flow-regime-dependent constitutive relations for wall shear specify momentum transfer between the fluid and the pipe surfaces.

The numerical solution method used is a staggered-mesh, semi-implicit, finite-difference method that is not transit-time-limited [Hanna *et al.* 1985]. Conservation of mass is achieved using a truncation error correction technique similar to that used in RELAP5 / MOD2 [Ransom 1983]. Mass conservation is particularly important in predicting 2-phase thermosiphoning because of its sensitivity to small changes in mass inventory. As well, the length of the transients makes them vulnerable to the accumulation of small errors, to a point where the solution is adversely affected.

Heat transfer from metal surfaces is handled by a complex wall heat transfer package. A set of flow-regime-dependent constitutive relations specify energy transfer between the fluid and the pipe wall and / or fuel element surfaces. Heat transfer by conduction within the piping and fuel is modelled in the radial direction and can be modelled in the circumferential direction as well. Radiative heat transfer and the zirconium-steam reaction can also be included. Built

Table 2: Summary of Test Conditions

Heated section power (kW)	*Secondary pressure (MPa)*	*Initial primary pressure (MPa)*	*Total inventory drained*	
			(L)	*% Loop volume*
160	4.6	7.1	291	30
80	4.6	7.1	271	30
60	0.2	5.1	486	50
160	0.2	5.1	583	60

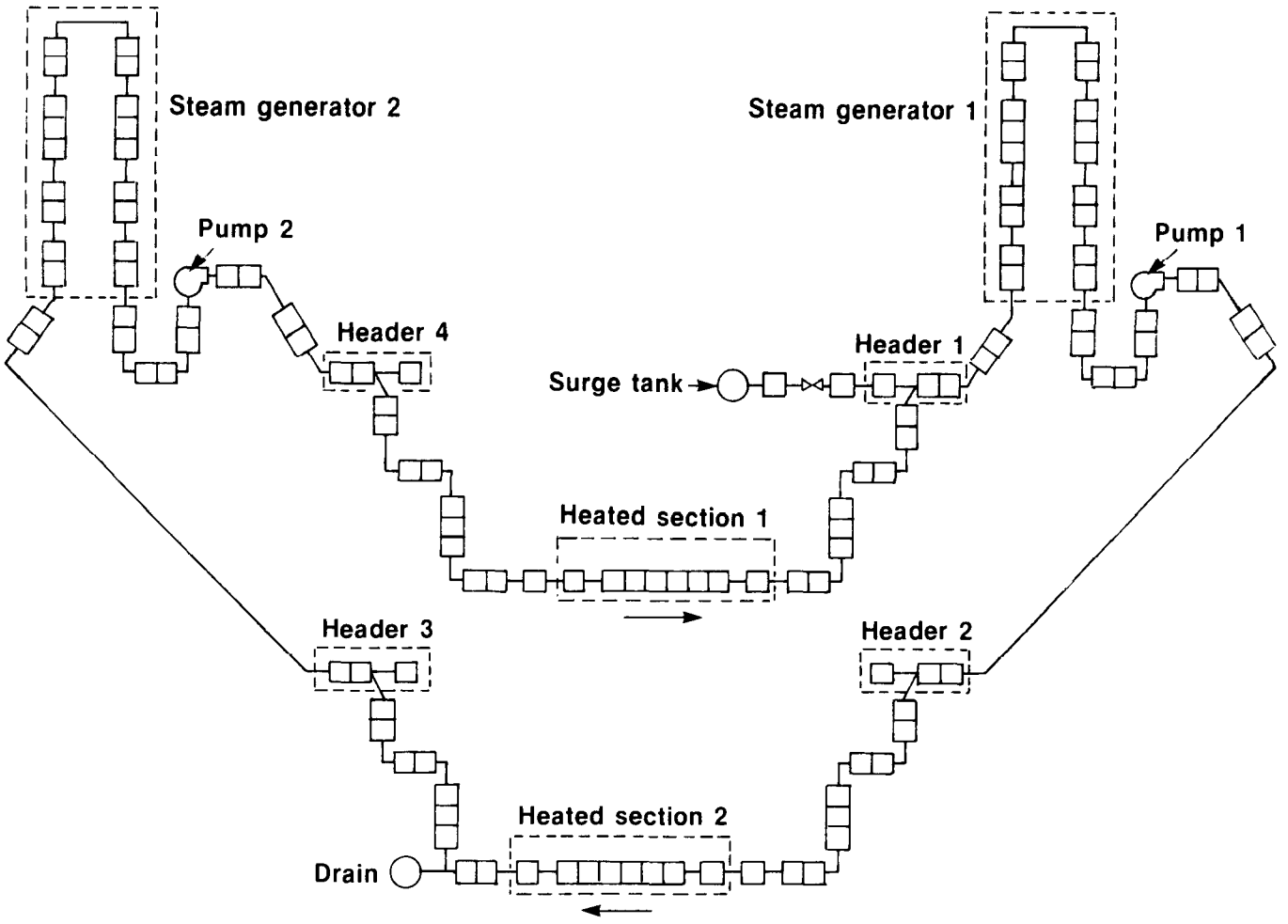

Figure 2 RD-14 primary side nodalization.

into this package is the ability to calculate heat transfer from individual groups of pins in a fuel bundle subjected to stratified flow. Under these conditions, the top pins in a bundle are exposed to steam while the bottom pins are exposed to liquid.

Component models which describe the behaviour of pumps, valves, steam separators, and discharge through breaks are available to complete the idealizations of reactor systems. A more complete description of the CATHENA code is available [Richards *et al.* 1985].

Nodalization

The nodalization used for these simulations is shown in Figure 2. A total of 130 nodes and 130 links were used to model the RD-14 facility. Modelling of the steam generators presented 2 problems which have been rectified. First, it was not clear what type of recirculation mode occurred within the steam generator secondary side. Normal full-power operation has fluid flow up the shell, with steam carried out of the top and liquid returning to the bottom of the shell via the downcomer. However, no recirculation via the external downcomer occurred, resulting in a 'kettle-like' operation of the steam generators in the tests described here. Rising 2-phase flow near the centre of the steam generators, and falling single-phase flow near the outer shell, was the probable mode of recirculation. This would have resulted in the outer tubes being exposed mainly to single-phase liquid and the inner tubes seeing a 2-phase mixture. To simplify the simulation it was assumed that all steam generator tubes experienced the same secondary side conditions of 2-phase boiling. An estimate of the heat transfer coefficient on the outer tube surfaces was made, based on detailed CATHENA steam generator simulations. All secondary side temperatures, except those in the preheater section of the steam generator, were assumed to be constant, and were set to the saturation temperature corresponding to the experimental secondary side pressure.

Second, 2 of the experiments showed evidence of unsteady feedwater flow in steam generator 2, which resulted in periodic drops in the primary fluid temperature exiting the steam generator, (see Figures 3 and 4). Since the predictions proved to be quite sensitive to these temperature drops, the boundary condition

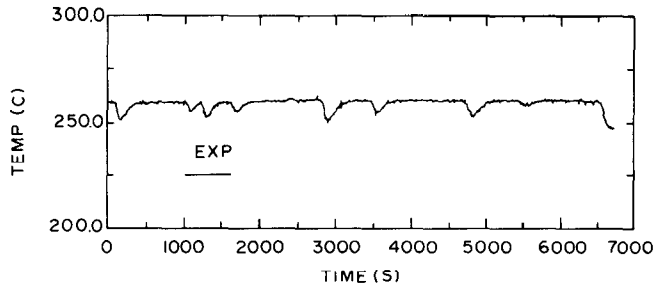

Figure 3 High-power, high-pressure case steam generator 2 – primary system outlet fluid temperature.

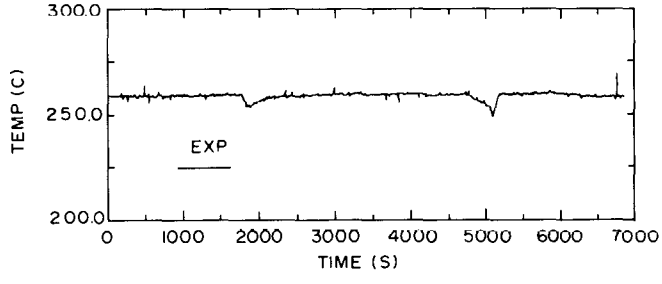

Figure 4 Low-power, high-pressure case steam generator 2 – primary system outlet fluid temperature.

temperature in the preheater section only was periodically adjusted to match the experimental observations.

Heat losses from the loop pipework to the environment were included in the analysis. Draining was simulated by an imposed intermittent flow of liquid from the outlet of heated section 2 into a boundary reservoir.

Results

The first 3 test conditions shown in Table 2 were simulated using CATHENA and are presented here. The primary loop inventory history of each test is shown at the beginning of each series of plotted results. Each fall in the level indicates a draining operation. A brief characterization of each experiment is followed by a comparison of the predicted and experimental parameters.

High-Power, High-Pressure Test

Figures 5 to 11, inclusive, show the simulation and experimental results for the high-power (160 kw / pass) and high-pressure (4.6 MPa) test. Generally this case is characterized by stable non-oscillating forward flow. Some small oscillations are evident for a brief period around 6,000 seconds. Near the end of the test, at loop inventories of about 70%, sufficient void penetrates the steam generators to cause reduced primary flow and stratification in the heated channels. The exposed top heater pins quickly heat up and trip the power on high temperature, terminating the experiment.

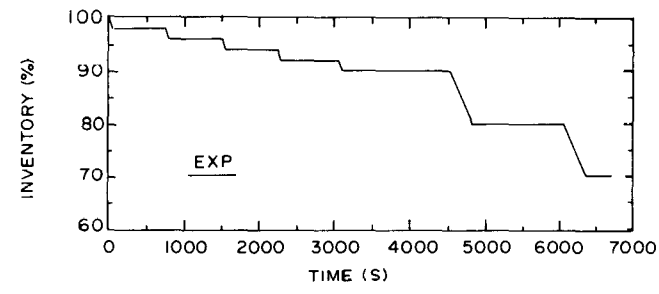

Figure 5 High-power, high-pressure case loop inventory (full 951.4 L).

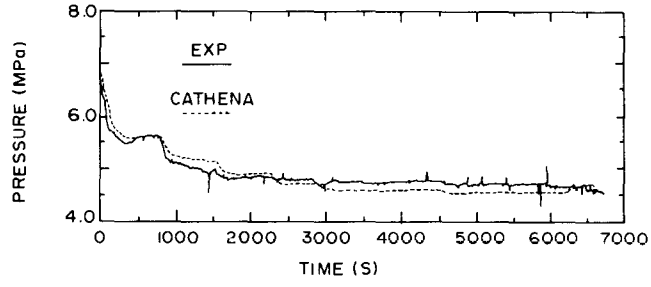

Figure 6 High-power, high-pressure case header 1 pressure.

The primary side pressure history at header 1 is shown in Figure 6. Generally, good agreement between the CATHENA simulation and the experimental results was achieved. A slight overestimation early in the transient is probably a result of small discrepancies in the initial fluid temperatures. The slight underestimation in pressure after 3,000 seconds is thought to result from overestimating the heat removal rate from the steam generators.

Figure 7 shows the volumetric flow at the inlet to test section 2. Only a slight underestimate in flow is seen until around 2,300 seconds. The prediction overestimates the primary flow beginning around 3,000 seconds. Up to this time, each draining operation has resulted in decreased system pressure and increased void. The increased void results in a higher driving

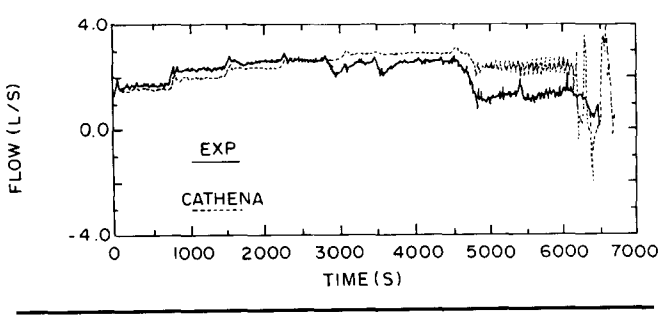

Figure 7 High-power, high-pressure case heated section 2 inlet flow.

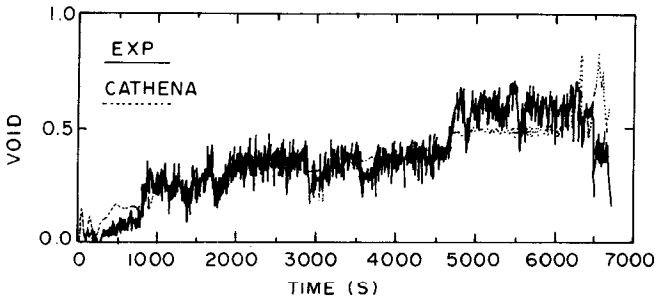

Figure 8 High-power, high-pressure case heated section 1 outlet void.

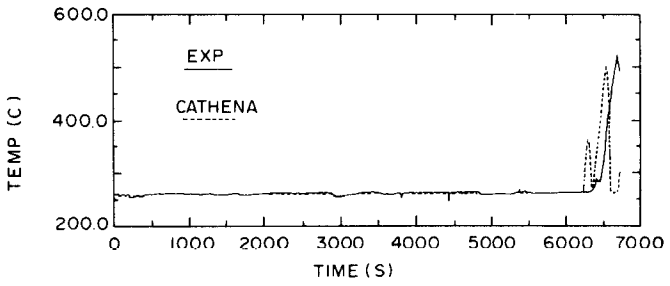

Figure 9 High-power, high-pressure case heated section 1 inlet – upper sheath temperature.

head, and therefore higher flowrates. Also, up to this time the void condensed completely in the riser side of the steam generator tubes. After 3,000 seconds, void was able to reach the top of the tubes and collect in the cold-leg side, thereby retarding the flow. An overestimate in the steam generator heat removal rate, mentioned previously, caused a delay in the timing of void carry over, resulting in the predicted flows being higher than the measured flows.

Oscillations in the CATHENA simulation started at 4,800 seconds. Small-amplitude oscillations commenced in the experiment at about 6,000 seconds.

Figure 8 shows the void fraction at the outlet of heated section 1. The predicted results agree well with the measured values until about 4,500 seconds, with only a slight overestimate in void in the first 900

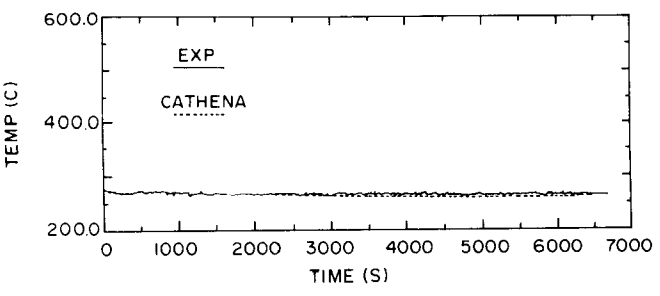

Figure 10 High-power, high-pressure case heated section 1 middle – lower sheath temperature.

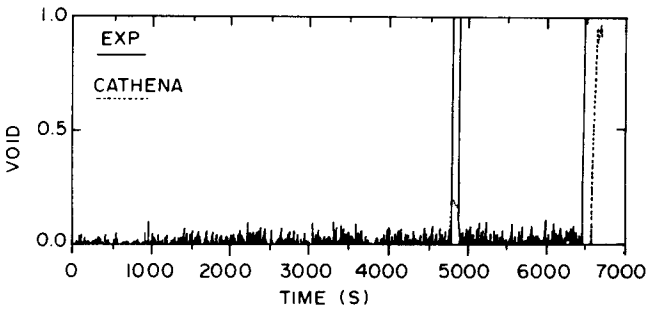

Figure 11 High-power, high-pressure case steam generator 1 outlet void.

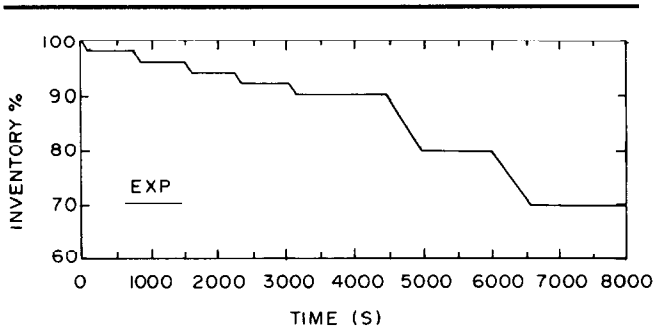

Figure 12 Low-power, high-pressure case loop inventory (full 954.1 L).

seconds. The CATHENA prediction underestimates the void after 4,500 seconds as a result of the high flows predicted in Figure 7.

Figures 9 and 10 show the heater pin sheath temperatures of the uppermost pin at channel 1 inlet, and a lower pin near the middle of channel 1, respectively. The effects of flow stratification were correctly captured in the CATHENA simulation. The code correctly predicted dryout of the top heater pin with no dryout of the lower pin. However, timing of dryout was slightly premature.

The void fraction history shown in Figure 11 is taken at the inclined outlet of steam generator 1. As previously mentioned, around 3,000 seconds void is able to penetrate the steam generators past the top of the tubes and begin collecting in the cold-leg side. The draining operation beginning at 4,500 seconds causes additional steam to be generated, 'flashing' in the piping between the heated section outlets and the steam generator. Unable to condense all of the entering vapour, the steam generator becomes flooded with steam, and in so doing retards the flow (see Figure 7). Figure 11 indicates that the steam generator first becomes steam-filled at 4,800 seconds. After the draining operation stops at about 4,800 seconds the system begins to stabilize and re-establish a more steady flow. The void returns to a low value, indicating that the steam-liquid interface has moved back up into the

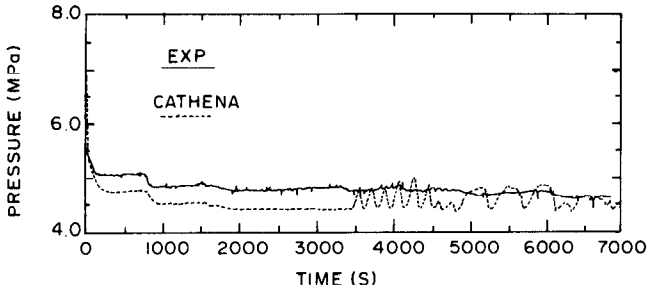

Figure 13 Low-power, high-pressure case header 1 pressure.

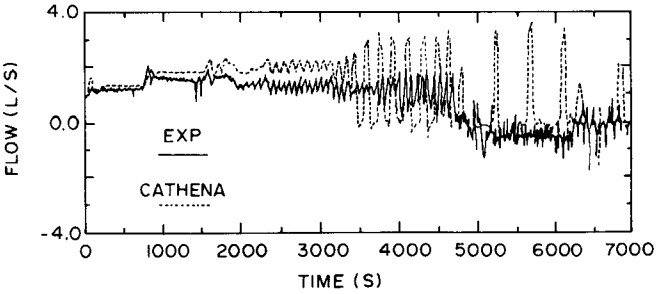

Figure 14 Low-power, high-pressure case heated section 2 inlet flow.

steam generator cold-leg side. CATHENA correctly predicted the occurrence of void at this time, but in insufficient quantities, again a result of high heat removal rates in the steam generator. The void spike after 6,400 seconds was predicted late in the simulation.

Low-Power, High-Pressure Test

Figures 12 through 18, inclusive, show the simulation and experimental results for the low-power (80 kw/pass) and high-pressure (4.6 MPa) case. This test, like the previous one, starts out in a stable non-oscillatory forward flow mode. Around 2,000 seconds, and at 94% loop inventory, small regular oscillations begin to appear and grow in amplitude as more primary fluid is drained. The flow oscillations occur in both halves of the loop and are almost in phase with one another. At about 4,600 seconds, and approximately 90% loop inventory, flow stagnation and fuel temperature excursions first occur. At 5,000 seconds, and at 80% loop inventory, a small less well defined oscillating negative flow develops which results in periodic dryout of the upper fuel elements. After 6,000 seconds, and at 70% loop inventory, the flow oscillates about a zero mean, the channel flow stratifies, and high pin temperature trip terminates the experiment.

The primary side pressure trace, Figure 13, shows the predicted pressure to be low up to 3,500 seconds. Since similar secondary side boundary conditions were used for this case as used in the high-pressure

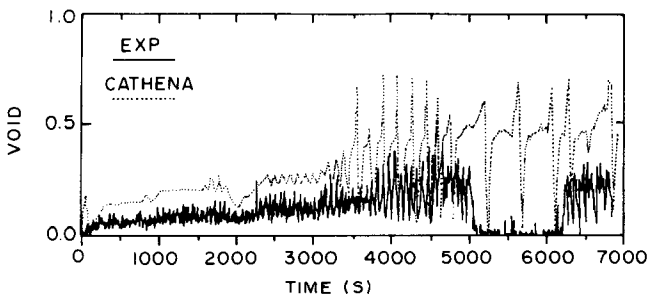

Figure 15 Low-power, high-pressure case heated section 1 outlet void.

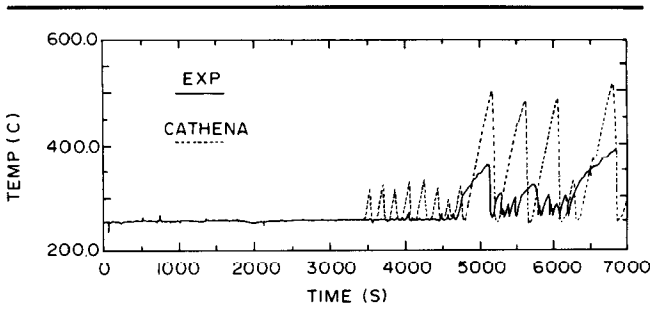

Figure 16 Low-power, high-pressure case heated section 1 inlet – upper sheath temperature.

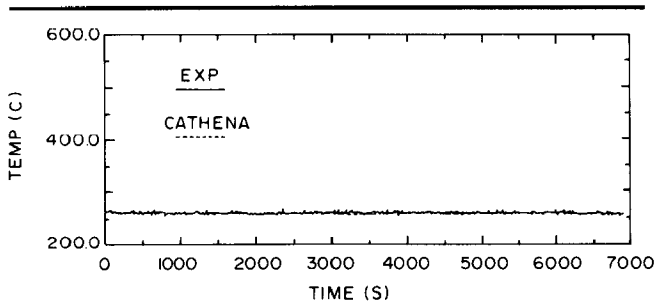

Figure 17 Low-power, high-pressure case heated section 1 middle – lower sheath temperature.

high-power case, excessive predicted heat removal in the steam generators is suspected. The effect is more pronounced because of the lower input power used in this experiment. After 3,500 seconds, pressure spikes are incorrectly predicted. They result from excessively large predicted flowrates and heater pin temperature oscillations.

Figure 14 shows the predicted flow to be high up to 3,200 seconds. The assumed high predicted heat removal rate from the steam generators results in a lower predicted system pressure, seen in Figure 13, and a higher predicted test section outlet void, seen in Figure 15, than occurred in the experiment. The increased void creates a higher driving head, and therefore higher flow rates, than those observed. The

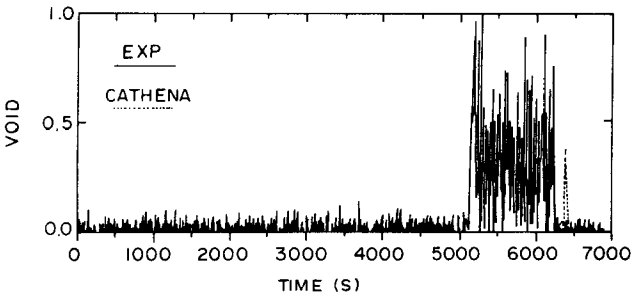

Figure 18 Low-power, high-pressure case steam generator 1 outlet void.

onset, amplitude, and period of the oscillations are, however, well predicted. After 3,200 seconds the predicted oscillations become much larger and longer in period than in the experiment. The reason for this discrepancy is thought to lie in the predicted higher voids, which cause a transition from bubbly flow to annular flow in the vertical pipe sections. This allows quicker movement of vapour to the steam generators where it accumulates and slows the flow. The resulting annular flow that develps in the steam generator tubes also reduces the condensation rate, thereby increasing the period of oscillation. It does this through a reduction in the vapour-to-liquid interface area. The relatively steady reverse flow, observed in the experiment between 5,000 and 6,000 seconds, was not predicted by CATHENA. The near stagnant conditions predicted were probably a result of the overestimation in void. The results of the draining operation after 6,000 seconds, which causes the flow to stagnate in the experiment, support this.

Shown in Figure 15 is the void fraction at the outlet of heated section 1. Generally, it shows higher outlet void than that observed in the experiment. As explained previously, the suspected high heat removal rate in the steam generators, which causes low system pressure to be predicted, is responsible. The single-phase liquid conditions seen in the experiment between 5,000 and 6,200 seconds result from the small reverse flow seen in Figure 14. The code predicted near stagnant conditions with occasional large brief positive flows, and, as a result, overestimates the amount of void present. After 6,200 seconds, the observed flow returns to near stagnant conditions and a sharp increase in void occurs.

The predicted heater pin sheath temperature shown in Figure 16 has numerous spikes beginning around 3,500 seconds. Intermittent dryout of the top heater pins is evident in the experiment around 4,000 seconds, but the temperature spikes tend to be much much smaller in amplitude. Again, this is caused by the large predicted flow oscillations that produce periods of flow stagnation in the channel. Dryout of the lower heater pin was correctly predicted not to occur (Figure 17).

Figure 18 shows the steam generator outlet void. In the experiment, the appearance of void at this location is a result of the flow reversal observed after 5,000 seconds. The void remains until 6,200 seconds because the small, steady, reverse flow persists until that time. Later, the void disappears as flow stagnation occurs. CATHENA predicted near-stagnant conditions, with periodic positive flow surges starting around 5,000 seconds, and therefore did not predict the appearance of void at this location. The spike predicted at 6,400 seconds resulted from void carried through the steam generator tubes by a positive surge in flow around 6,300 seconds (see Figure 14). Previous flow surges at 5,200, 5,600, and 6,100 seconds flooded the steam generators with steam, but during the periods of stagnant flow between surges the steam generators were able to condense the steam. The surge in flow at 6,300 seconds follows shortly after the surge at 6,100 seconds, and the steam generator was not able to recover sufficiently from the previous flow surge.

Low-Power, Low-Pressure Test

Figures 19 through 25, inclusive, show the simulation and experimental results for the low-power (60 kw / pass) and low-pressure (0.2 MPa) test. In this test an intermittent flow pattern develops early at about 98% of loop inventory. Large, nearly in-phase flow surges

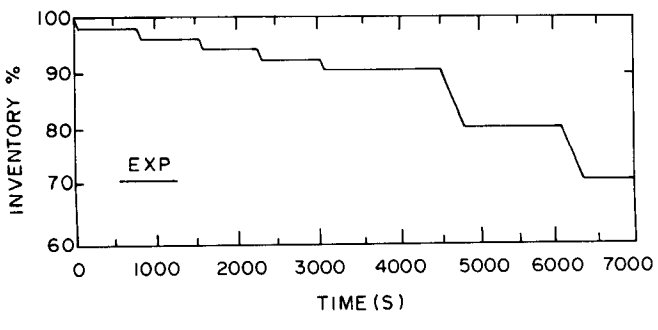

Figure 19 Low-power, low-pressure case loop inventory (full 954.1 L).

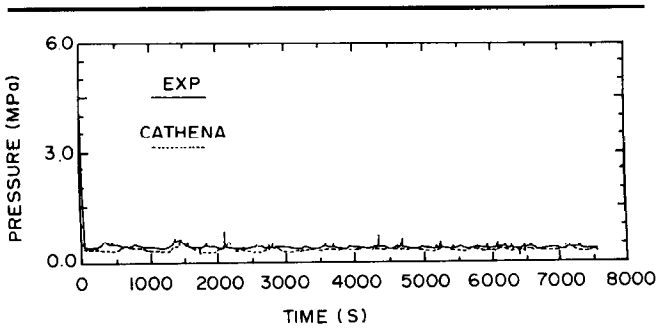

Figure 20 Low-power, low-pressure case header 1 pressure.

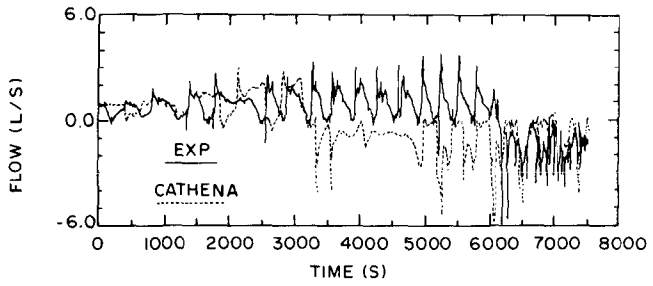

Figure 21 Low-power, low-pressure case heated section 2 inlet flow.

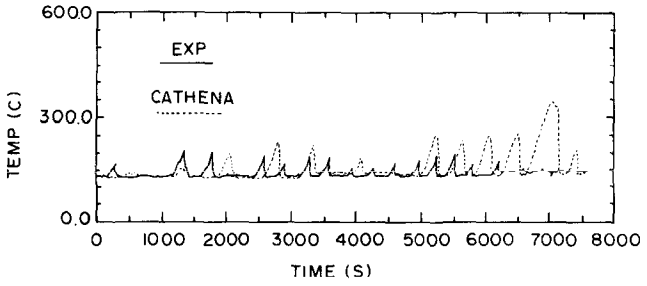

Figure 23 Low-power, low-pressure case heated section 1 inlet – upper sheath temperature.

from near-stagnant conditions were observed in both halves of the primary circuit. This allowed periodic dryout of the upper fuel elements. With each successive draining operation, the period of the oscillations shortened. At loop inventories of about 70% the mean flow direction reversed, and less well defined negative flow oscillations developed. Finally, at 50% of primary loop inventory, flow stagnation occurs, resulting in a power supply trip on high heater pin temperature and termination of the experiment.

The predicted primary pressure shown in Figure 20 shows good agreement with the experimental pressure. Only a small underestimation of the pressure and some discrepancies in timing of the pressure oscillations are seen in the CATHENA simulation.

Figure 21 shows the predicted flow oscillations, up to 3,400 seconds, have the correct general shape and amplitude but a longer period. In addition, the flow reversal observed in the experiment after 6,000 seconds is prematurely predicted to occur at about 3,400 seconds. Since these cases are very sensitive to the amount and distribution of void, especially in the vertical pipe legs, it is important to predict correctly condensation within the steam generators. Large primary side oscillations can be expected to induce void and flow oscillations in the secondary side which affect the heat removal rate from the primary side. The simple modelling of the secondary side used in these simulations is again suspected of being inadequate in this case.

Shown in Figure 22 is the void fraction at the outlet of heated section 1. The oscillations up to 3,400 seconds tend to have much longer periods than those observed in the experiment, as a result of the longer period flow oscillations predicted by CATHENA. During the time period from 3,400 to 5,000 seconds the predicted reverse flow removes any void from this location. Once periodic stagnant flow is again predicted, starting after 5,000 seconds, spikes in void reappear. After 6,000 seconds the flow reverses in the experiment and is maintained with only brief periods of stagnant flow. As a result, no spikes in void appear. The prediction shows void spikes because the flow is predicted to stagnate for much longer periods of time.

The sheath temperature of the upper heater pin, Figure 23, shows that the predicted oscillations, before the predicted flow reversal at 3,400 seconds, have the correct amplitude but a longer period than in the experiment. After 5,000 seconds large temperature excursions due to the long periods of stagnated flow are predicted. Unlike in the previous two test cases, the lower pin location, plotted in Figure 24, approaches dryout conditions. This is predicted well by CATHENA.

The steam generator outlet void fraction plot, Figure 25, shows that the arrival of void, at 3,600 seconds in

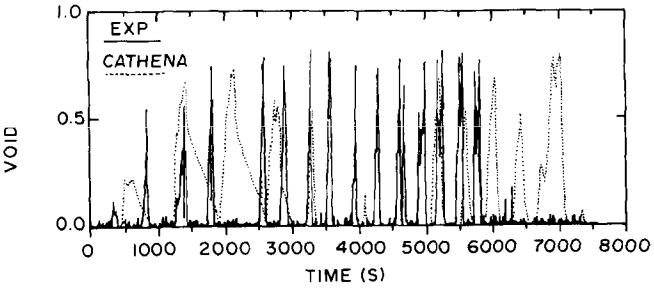

Figure 22 Low-power, low-pressure case heated section 1 outlet void.

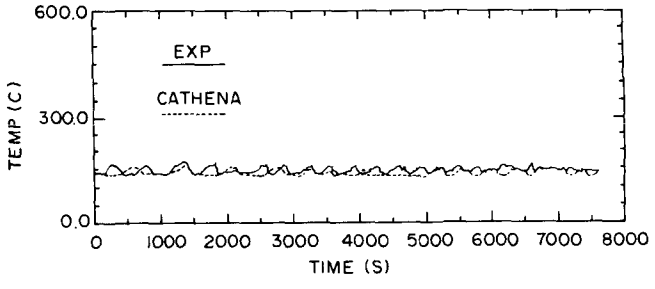

Figure 24 Low-power, low-pressure case heated section 1 middle – lower sheath temperature.

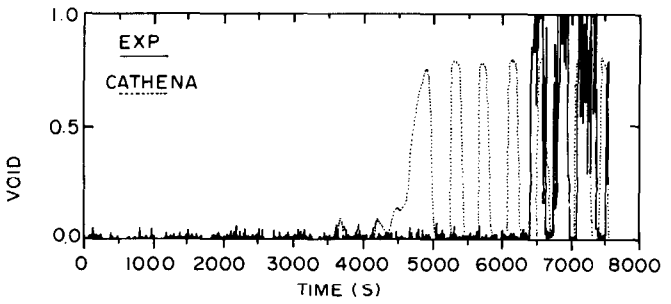

Figure 25 Low-power, low-pressure case steam generator 1 outlet void.

the simulation, occurred shortly after a negative flow was predicted. The experiment also shows the arrival of void after a negative flow developed, but not until 6,400 seconds.

Conclusions

The CATHENA code has been used to predict thermosiphoning tests conducted in the RD-14 thermalhydraulic test facility. In the tests simulated, the code has correctly predicted the occurrence of non-oscillating and oscillating 2-phase thermosiphoning flow behaviour.

Non-oscillating 2-phase thermosiphoning flow and the timing of the onset of oscillations are well predicted. The use of constant boundary conditions for the steam generator secondary side is adequate for these conditions.

Oscillating 2-phase thermosiphoning flow is not as well predicted. The predicted period tends to be longer and the amplitude exaggerated. For this type of flow, constant boundary conditions for the steam generator secondary side may not be adequate. Where the period of oscillation is long and the oscillation amplitude large, the interaction between the primary and secondary side appears to be important.

In all cases, the differing behaviour of the upper and lower pins was captured in the predictions. In the presence of stratified flow upper elements became exposed to steam and experienced temperature excursions, while the lower elements remained cooled by single-phase liquid.

Acknowledgements

The experiments presented in this paper were funded by the CANDU Owners Group (COG).

This paper is a revised and expanded version of a paper originally presented at the Second International Conference on Simulation Methods in Nuclear Engineering, Montreal, 14–16 October 1986.

Notes and References

1. *Hanna BN*, et al. One-step semi-implicit method for solving the transient two-fluid equations that is non-courant limited. 11th National Heat Transfer Conference, Denver, 1985.
2. *Krishnan VS, Gulshani P* Thermosiphoning behaviour of a pressurized-water facility with CANDU PHTS geometry. Presented at the 2nd International Topical Meeting on Nuclear Power Plant Thermalhydraulics and Operations, Tokyo, 1986.
3. *Ransom VH.* RELAP / MOD2: for PWR transient analysis. In: CNS / ANS International Conference on Numerical Methods in Nuclear Engineering. Montreal, 1983: 40–60.
4. *Richards DJ*, et al. ATHENA: a two-fluid code for CANDU LOCA analysis. Presented at the Third International Topical Meeting on Reactior Thermalhydraulics, Newport, Rhode Island, 1985.